


Article

Pan-Genome-Wide Identification and Transcriptome-Wide Analysis of ZIP Genes in Cucumber

Zimo Wang¹, Mengmeng Yin¹, Jing Han², Xuehua Wang¹, Jingshu Chang¹, Zhonghai Ren¹  and Lina Wang^{1,*}

¹ Shandong Collaborative Innovation Center of Fruit & Vegetable Quality and Efficient Production, College of Horticultural Science and Engineering, Shandong Agricultural University, Tai'an 271018, China; 2021110304@sda.u.edu.cn (Z.W.); 2021110287@sda.u.edu.cn (M.Y.); 2022110315@sda.u.edu.cn (X.W.); 2022110303@sda.u.edu.cn (J.C.); zhren@sda.u.edu.cn (Z.R.)

² College of Agriculture and Agricultural Engineering, Liaocheng University, Liaocheng 252000, China; hanjing@lcu.edu.cn

* Correspondence: lnwang@sda.u.edu.cn

Abstract: The ZRT/IRT-like proteins (ZIPs) play critical roles in the absorption, transport, and intracellular balance of metal ions essential for various physiological processes in plants. However, little is known about the pan-genomic characteristics and properties of ZIP genes in cucumber (*Cucumis sativus* L.). In this study, we identified 10 CsZIP genes from the pan-genome of 13 *C. sativus* accessions. Among them, only CsZIP10 showed no variation in protein sequence length. We analyzed the gene structure, conserved domains, promoter *cis*-elements, and phylogenetic relationships of these 10 CsZIP genes derived from "9930". Based on phylogenetic analysis, the CsZIP genes were classified into three branches. Amino acid sequence comparison revealed the presence of conserved histidine residues in the ZIP proteins. Analysis of promoter *cis*-elements showed that most promoters contained elements responsive to plant hormones. Expression profiling in different tissues showed that most CsZIP genes were expressed at relatively low levels in *C. sativus* leaves, stems, and tendrils, and CsZIP7 and CsZIP10 were specifically expressed in roots, indicating their potential involvement in the absorption and transport of metal ions. Transcriptomic data indicated that these 10 ZIP genes displayed responses to both downy mildew and powdery mildew, and CsZIP1 was significantly downregulated after both salt and heat treatments. In conclusion, this study deepens our understanding of the ZIP gene family and enhances our knowledge of the biological functions of CsZIP genes in *C. sativus*.

Keywords: gene identification; *Cucumis sativus*; CsZIP



Citation: Wang, Z.; Yin, M.; Han, J.; Wang, X.; Chang, J.; Ren, Z.; Wang, L. Pan-Genome-Wide Identification and Transcriptome-Wide Analysis of ZIP Genes in Cucumber. *Agriculture* **2024**, *14*, 133. <https://doi.org/10.3390/agriculture14010133>

Academic Editor: Rodomiro Ortiz

Received: 2 January 2024

Revised: 13 January 2024

Accepted: 14 January 2024

Published: 16 January 2024



Copyright: © 2024 by the authors. Licensee MDPI, Basel, Switzerland. This article is an open access article distributed under the terms and conditions of the Creative Commons Attribution (CC BY) license (<https://creativecommons.org/licenses/by/4.0/>).

1. Introduction

The homeostasis of metal ions plays a crucial role in the growth and development of plants. Appropriate concentrations of metal ions are required by plants to sustain biochemical reactions and physiological processes within cells. However, an excess or deficiency of metal ions may lead to severe growth issues and physiological disruptions. Therefore, maintaining suitable concentrations of metal ions is vital for the survival of plants. The ZIP gene family performs a significant role in the metal ion homeostasis of plants. This family encodes the zinc ion transport proteins responsible for regulating the absorption and distribution of zinc as well as other metal ions. Through the activity of these proteins, plants can respond to changes in environmental metal ion levels and maintain a balanced state of metal ions within cells [1,2]. Most ZIP proteins consist of 309–476 amino acid residues and possess eight putative transmembrane (TM) domains. They exhibit a common membrane topology, with the N- and C-terminal ends located extracytoplasmically [3]. The cytoplasmic loop between TM3 and TM4 contains a histidine-rich domain (HRD), which functions as the metal binding domain involved in metal transport. Additionally, the

amphipathic nature of TM5 and TM4 creates a cavity that allows for the passage of metal ions [2,3].

Currently, more than 300 members of the ZIP protein family have been identified from plants, and the function of some ZIP members has been identified. The ZIP gene, *AtIRT1*, was first identified in *Arabidopsis thaliana*. It encodes an iron transporter protein and is mainly expressed in the roots [4]. The previous study has shown that *AtIRT1* also exhibits specific expression in the companion cells of the cortex and plays a role in iron transport in aerial organs [5]. *AtIRT2* is another IRT gene that functions similarly to *AtIRT1* in *A. thaliana*. *AtIRT2* is located on the vacuole membrane and transports Fe to the vacuole to prevent it from being poisoned in the cytoplasm [6]. *AtZIP1* and *AtZIP3* are mainly expressed in roots. *AtZIP1* is a vacuolar transport protein that transports Zn/Mn from the root cells to the cytoplasm [7]. *AtZIP3* functions in the uptake of Zn and Fe in plant roots [2].

AtZIP2 promotes Mn/Zn uptake and transport in xylem parenchyma cells, thereby facilitating the transport of Mn/Zn towards the shoots [7]. In contrast, *AtZIP4* transports metal ions into plant cells or between tissues [2]. In addition, some ZIP transporter proteins directly participate in the enrichment of Zn in edible parts [8,9]. The expression levels of the ZIP gene family in plants exhibit dynamic changes. For example, under zinc deficiency conditions, the expression levels of some ZIP transport proteins increase. However, when zinc levels return to normal or increase, their expression levels decrease [10].

In rice (*Oryza sativa* L.), *OsIRT1* and *OsIRT2* are iron-transport proteins that directly absorb Fe^{2+} and Zn^{2+} into root cells [11–14]. When *O. sativa* is exposed to iron deficiency conditions, the expression of *OsIRT1* and *OsIRT2* in the root system is upregulated [15]. *OsZIP1* is located in the plasma membrane. Under the condition of excessive metal ions, *OsZIP1* plays a role as a transporter in *O. sativa* [16]. Furthermore, studies have shown that the overexpression of *OsZIP1* can increase the accumulation of metal ions in plant tissues [13,14]. *OsZIP4* and *OsZIP5*, as plasma membrane-localized Zn transporters, participate in Zn^{2+} uptake in *O. sativa* [17,18]. Overexpression of *OsZIP4* and *OsZIP5* can increase the content of Zn^{2+} in plants [17,18]. *OsZIP8* is also a Zn transporter protein in *O. sativa*, participating in the uptake and distribution of Zn^{2+} [19]. Generally speaking, ZIP transport proteins are primarily involved in the absorption and transport of Zn and Fe. However, these proteins also play a role in the absorption of other metal ions, such as Cu and Mn [7].

Additionally, they can also participate in the transport and absorption of a variety of toxic metals, such as cadmium (Cd), in plants [20]. For example, overexpression of *OsIRT1* in *O. sativa* has been found to enhance its resistance to Cd [21]. *ZIP2* and *ZIP3* have been demonstrated the involvement in the uptake and transport of Cd in cabbage, with an increase in their expression levels [22]. In tomato (*Solanum lycopersicum* L.), the expression of *SZIP4* is positively correlated with content of Cd within a specific range [23]. Additionally, ZIP genes also participate in the absorption and transport of Cd in mulberry and tobacco [24,25].

In recent botanical studies, one of the core issues of concern is the mechanism of plant tolerance to biotic and abiotic stresses. In barley, 3029 up-regulated genes and 3017 down-regulated genes involved in drought tolerance were successfully identified [26]. In Qingke (*Hordeum vulgare* L. var. nudum), drought induced the expression of *HOVUSG1548800*, *HOVUSG2056400* and *HOVUSG5062900* [27]. In tea plant (*Camellia sinensis* L.), most ZIP genes are involved in the response of tea to abiotic stress. Under NaCl treatment, the expression of *ZIP1*, *ZIP6*, *ZIP9*, *ZIP11*, and *ZIP12* genes decreased. Under cold stress, *ZIP1*, *ZIP3*, *ZIP6*, *ZIP7*, *ZIP11*, and *ZIP12* genes were up-regulated. Under MeJA treatment, the transcription level of *ZIP4* decreased [28].

In *H. vulgare*, *HOVUSG6558000*, *HOVUSG5063500*, *HOVUSG5062800*, and *HOVUSG5062900* were identified as the main response genes to powdery mildew infection [27]. In sweet potato (*Ipomoea batatas* L.), according to bioinformatics analysis and RT-qPCR analysis, *IbNBS75*, *IbNBS219*, and *IbNBS256* were found to respond to stem nematode infection [29]. In *Arachis duranensis*, the expression level of *AdLTPs* changed. Three *AdLTPs* are

associated with resistance to nematode infection, and *DOF* and *WRI1* transcription factors may regulate the response of *AdLTP* to nematode infection [30].

Due to relatively limited research on the *ZIP* gene family in both abiotic and biotic stress conditions, it is crucial to investigate the role of the *ZIP* gene family in non-biological and biological stress to enhance our understanding of its internal functionalities.

Previous studies have reported the pan-genomic analysis of the *ZIP* gene family in different plants including *A. thaliana*, peanut, and *Populus trichocarpa*. *Arabidopsis* had 15 *ZIP* members, peanut 30, and *Populus trichocarpa* 16 [31–33]. However, there is no report on the *CsZIP* gene family yet in *C. sativus*. Therefore, it is necessary to analyze the *CsZIP* gene family.

C. sativus is a popular cash crop due to its unique flavor and refreshing crisp texture [34]. Due to the crucial role of the *CsZIP* gene family in the absorption and transportation of metal ions, and in order to explore the function of *ZIP* gene family in abiotic and biotic stresses, it is imperative to analyze and identify the *CsZIP* gene family in *C. sativus*. The updated genome database of *C. sativus* provides a better resource for identifying and characterizing *CsZIP* genes. In this study, bioinformatics methods were used to study the sequence similarity, gene structure, and expression pattern of *CsZIP* gene family, aiming to deepen the understanding of *CsZIP* gene and improve the understanding of its biological function.

2. Materials and Methods

2.1. Identification of ZIP Genes in *C. sativus*

The analysis and identification of *ZIP* genes in *C. sativus* were conducted by utilizing the genome sequence data available on the Cucurbit Genomics Data website (<http://cucurbitgenomics.org/organism/20> (accessed on 1 January 2023)). The hidden Markov model (HMM) profile files of the *ZIP* conserved domain (PF02535) were downloaded from the Pfam database (<http://pfam.xfam.org/> (accessed on 3 January 2023)). The *ZIP* gene was searched from the *C. sativus* genome database using HMMER 3.0, and the default parameter and cutoff value were 0.01. The Pfam tool (<http://pfam.janelia.org> (accessed on 5 January 2023)) and SMART (<http://smart.embl-heidelberg.de/> (accessed on 5 January 2023)) were employed for confirming the conserved domain of *ZIP*. The prediction of *ZIP* candidates was conducted through the ExpASY Proteomics Server as described by Artimo et al. in 2012. Subsequently, the subcellular localization of the protein was analyzed using the Cell-PLoc tool [35].

2.2. Motif Analysis and Gene Structure

The CDS sequences and genomic data for *CsZIP* genes retrieved from the *C. sativus* genome database (<http://cucurbitgenomics.org/organism/20> (accessed on 1 February 2023)) were visualized using the Gene Structure Display Server online tool (<http://gsds.cbi.pku.edu.cn/> (accessed on 1 February 2023)) [36]. The conserved motifs of *CsZIP* proteins were then identified with MEME 4.9.1 (<http://meme-suite.org/> (accessed on 1 February 2023)) [37] and visualized with WebLogo (<http://weblogo.berkeley.edu/logo.cgi> (accessed on 1 February 2023)) [38]. The total number of motifs (nmotifs) is 10, the minimum length of motifs (minw) is 6 amino acids, and the maximum length of motifs (maxw) is 10 amino acids.

2.3. Phylogenetic Analysis and Multiple Sequence Alignment

The MEGA software (v7.0) was utilized to align the protein sequences of *ZIP* from *A. thaliana*, *C. sativus*, melon, and *O. sativa* using the ClustalW algorithm. Subsequently, the evolutionary relationship between *ZIP* proteins was analyzed using the neighbor-joining method software, and the number of repetitions was 1000 times. The resulting phylogenetic trees underwent graphical representation and enhancement through Evolview (<https://evolgenius.info/evolview-v2/#login> (accessed on 3 February 2023)).

2.4. Gene Duplication Analysis and Genome Distribution

The CsZIP loci, obtained from the *C. sativus* genome database (<http://cucurbitgenomics.org/organism/20> (accessed on 4 February 2023)), were visualized on chromosomes using MapChart software (MapChart 2.32) [39]. From Orthomcl [40], the homology of ZIP gene between *C. sativus* and *A. thaliana*, *Cucumis melo*, and *O. sativa* were obtained. Circos shows the chromosomal location and collinearity of the ZIP gene [41]. The comparison between all coding sequences (CDS) from Arabidopsis and *C. sativus* genomes was conducted using Clustal W. Subsequently, repeated pairs and homologous pairs were identified based on the alignment result. The Computational Biology Unit (CBU) Ka/Ks calculation tool was then utilized to compute the non-synonymous (Ka) and synonymous (Ks) nucleotide substitution rates. The divergence times of the duplicated genes were calculated using the formula $T = Ks/2r$ Mya (millions of years), where r equals 1.5×10^{-8} [42].

2.5. Analysis of Promoter Regions of CsZIP Genes

The 1.5-kb sequences upstream of the initiation codons (ATG) of CsZIP genes were obtained from the cucurbit genomics data website (<http://cucurbitgenomics.org/organism/20> (accessed on 5 February 2023)), and analyzed for cis-elements in the promoter region using the online tool PlantCARE [43].

2.6. Analysis of Transcriptome Data

The data from different *C. sativus* RNA-seq libraries were obtained from the Cucurbit Genomics Data website (<http://cucurbitgenomics.org/organime/20> (accessed on 3 March 2023)) and NCBI SAR databases (accession numbers: PRJNA388584, GSE151055, GSE81234, and GSE11265). The expression profile of CsZIP gene was visualized using TBtools software (v2.031) [44].

2.7. Plant Materials and Growth Conditions

In this study, the temporal and spatial expression patterns of ZIP genes were analyzed using the *C. sativus* inbred line “China long” 9930 (North China type). *C. sativus* were grown in greenhouses at Shandong Agricultural University in China, following standard water management and pest control practices.

2.8. RNA isolation and Real-Time PCR Analysis

To collect samples for expression analysis, the roots, stems, leaves, female and male flowers, ovaries, and tendrils of *C. sativus* plants were collected. These samples were immediately frozen in liquid nitrogen and stored at -80 °C for RNA isolation. Total RNA extraction was performed using TRIzol according to the manufacturer’s instructions, followed by DNase I treatment to eliminate potential DNA contamination. Subsequently, cDNA synthesis was conducted using the RevertAid First Strand Synthesis Kit. Primer sequences for the selected genes were designed using Primer Premier 5.0 (Table S4), with the *C. sativus* actin gene serving as an internal control. qRT-PCR validation of the selected genes was carried out using the Ultra SYBR Green Mixture qPCR kit (CW BIO, Beijing, China) on an iCycler iQTM real-time PCR detection system. The relative expression levels of the selected genes were determined using the $2^{-\Delta\Delta C_t}$ method [45].

3. Results

3.1. Identification of CsZIP Genes from *C. sativus* Pan-Genome

With the release of a graph-based pan-genome [46], we could identify ZIP genes in *C. sativus* by analyzing 13 accession genomes. We obtained the HMM configuration profile files and extracted CsZIP proteins from the *C. sativus* genome database. The candidate genes were further analyzed using NCBI, Pfam, and SMART. As a result, a total of 10 CsZIP genes were identified in the 13 *C. sativus* accessions (Table 1). Of these accessions, only “Cuc80” and “PI183967” contain nine CsZIP genes (Table 2). To avoid confusion, we renamed these genes as CsZIP1–CsZIP10 based on their chromosomal order (Table 3).

Table 1. The origins of the different *C. sativus* accessions.

Accession Name	Accession Group	Accession Name	Accession Group
9930	East Asian cultivated accession	Hx117	Indian cultivated accession
XTMC	East Asian cultivated accession	Hx14	Indian cultivated accession
Cu2	East Asian cultivated accession	W4	Indian wild accession
Cuc37	Eurasian cultivated accession	W8	Indian wild accession
Gy14	Eurasian cultivated accession	Cuc64	Indian wild accession
9110gt	Eurasian cultivated accession	PI183967	Indian wild accession
Cuc80	Xishuangbanna cultivated accession		

Table 2. The protein lengths of CsZIPs in different *C. sativus* accessions.

Protein Name	9930	XTMC	Cu2	Cuc80	Cuc37	Gy14	9110gt	PI183967	Cuc64	W4	W8	Hx14	Hx117
CsZIP1	249	350	350	-	350	350	350	350	350	350	350	350	350
CsZIP2	417	417	417	417	417	441	417	417	417	417	417	408	417
CsZIP3	228	275	275	275	275	306	275	275	306	275	275	275	275
CsZIP4	594	594	639	594	594	594	594	594	594	594	594	594	594
CsZIP5	367	367	367	365	367	367	367	367	369	367	365	369	815
CsZIP6	463	463	463	463	463	407	463	463	463	463	463	463	463
CsZIP7	335	335	335	335	335	335	335	335	335	302	335	335	346
CsZIP8	349	349	349	349	349	349	349	349	349	349	349	349	1096
CsZIP9	334	334	334	334	334	337	334	-	338	334	334	334	337
CsZIP10	354	354	354	354	354	354	354	354	354	354	354	354	354

Table 3. CsZIP family in *C. sativus*.

Gene	Introns	Chromosomal Site	Gene Length	Protein Length	Protein MW (kDa)	Isoelectric Point	Subcellular Location Predicted
CsZIP1	2	1	2955	249	27.2	6.88	Cell membrane
CsZIP2	3	2	3491	417	44.5	6.09	Chloroplast
CsZIP3	9	4	9406	228	24.6	7.02	Cell membrane
CsZIP4	4	4	5063	594	62.0	6.27	Cell membrane
CsZIP5	2	4	2777	367	38.8	5.98	Cell membrane
CsZIP6	10	5	21,173	463	49.9	5.97	Cell membrane
CsZIP7	1	6	2038	334	35.7	5.73	Chloroplast
CsZIP8	0	6	1490	348	38.0	5.58	Cell membrane
CsZIP9	2	7	7007	334	35.9	6.02	Cell membrane
CsZIP10	2	7	4076	354	37.2	8.53	Cell membrane

To further investigate the variation in CsZIP genes among different *C. sativus* accessions, we counted the length of the identified CsZIP proteins (Table 2). Among the 13 *C. sativus* accessions, only one gene, CsZIP10, had the same protein length across all accessions. The lengths of CsZIP1, CsZIP4, CsZIP6, and CsZIP8 differed in only one accession. CsZIP2, CsZIP3, and CsZIP7 exhibited variations in protein length in two accessions. CsZIP9 showed protein variations in three accessions, while CsZIP5 exhibited protein length differences in multiple accessions. All CsZIP protein sequences can be found in Dataset S2.

3.2. Characterization of CsZIP Genes from Chinese Long 9930

Subsequent analyses primarily focused on the genes identified in the '9930' genome, as it encompassed all the 10 CsZIPs and is the first *C. sativus* genome sequenced and has been updated to the V3 version. The gene name, gene number, gene intron number, chromosome position, gene length, protein length, isoelectric point, relative molecular

weight, and subcellular localization prediction of CsZIPs are presented in Table 3. Sequence analysis revealed that the length of CsZIP proteins ranged from 228 to 594 amino acids, with molecular weights ranging from 27.20 to 61.98 kDa. The longest and most complex gene structure was found in *CsZIP6*, while the shortest gene was *CsZIP8*. *CsZIP4* had the highest relative molecular weight, whereas *CsZIP3* the lowest. The isoelectric points of these proteins ranged from 5.58 to 8.53. Furthermore, subcellular localization prediction indicated that most CsZIP proteins were localized to the cell membrane, except *CsZIP2* and *CsZIP7*, which were found in the chloroplasts (Table 3).

3.3. Analysis of Phylogenetic Relationship and Gene Structure and Protein Motif

To analyze the phylogenetic relationship of CsZIP proteins, we constructed the phylogenetic tree of these 10 proteins (Figure 1). Based on the phylogenetic tree, the CsZIP family exhibited division into three distinct clades. Specifically, *CsZIP2*, *CsZIP5*, and *CsZIP10* were grouped within the first clade, *CsZIP8* and *CsZIP1* were positioned in the second clade, while the remaining CsZIPs were categorized under the third clade (Figure 1). The number of introns varied among *CsZIP* genes, ranging from 0 to 10: *CsZIP6* has the most introns, and *CsZIP8* has none (Figure 1). The structures of the *CsZIP6*, *CsZIP3*, and *CsZIP4* genes were similar, suggesting they are more closely related (Figure 1).

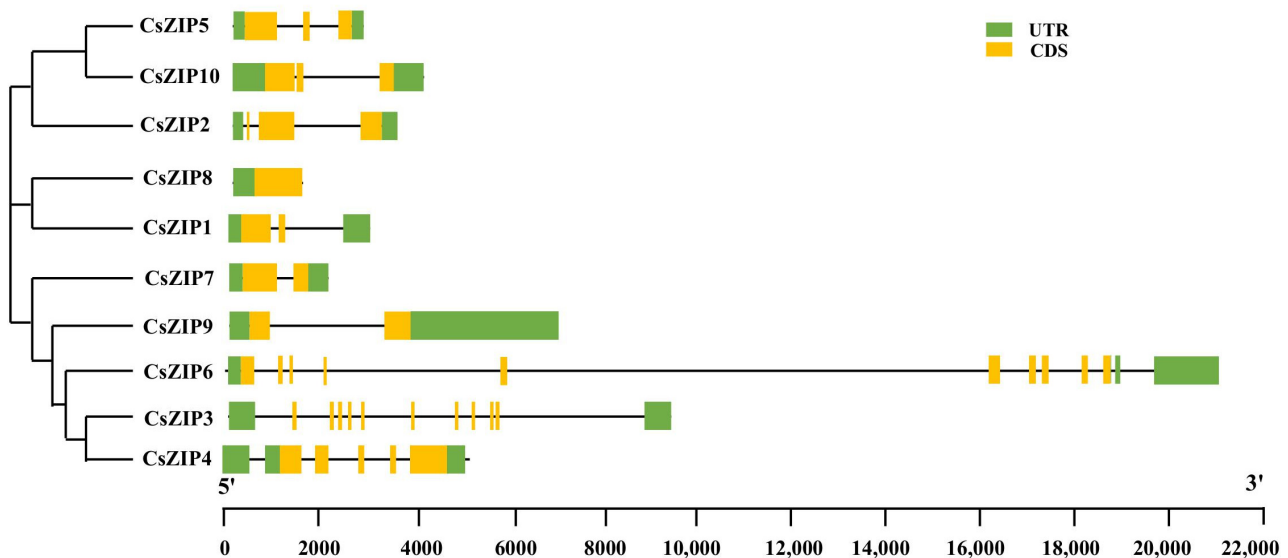


Figure 1. Phylogenetic tree and gene structure of ZIP family members in *C. sativus*. The phylogenetic tree was constructed using the neighbor-joining (NJ) method with 1000 bootstrap replicates, based on the alignment of the identified 10 ZIP proteins in *C. sativus*. The gene structures of the identified 10 ZIP genes in *C. sativus* were generated utilizing the Gene Structure Display Server v.2.0. In the structures, the green box represents the UTR, the yellow box represents the exon, and the black line represents the intron.

We further analyzed the conserved motifs of CsZIP family and found that motif type and arrangement were very similar among the members of the first and second clades, in all of which only motif 9 was present, but diverse among the members of the third clade, and motif number ranged from one (*CsZIP3* and *CsZIP4*) to seven (*CsZIP7*) (Figure 2). Motif 2 was present in all the CsZIPs except *CsZIP3*, indicating that motif 2 is highly conserved (Figure 2). *CsZIP6*, *CsZIP3*, and *CsZIP4* are the CsZIP proteins that did not contain motif 1 (Figure 2). The variations in motifs among CsZIP proteins could potentially account for their functional diversity. The amino acid sequence for each motif is presented in the Figure S1.

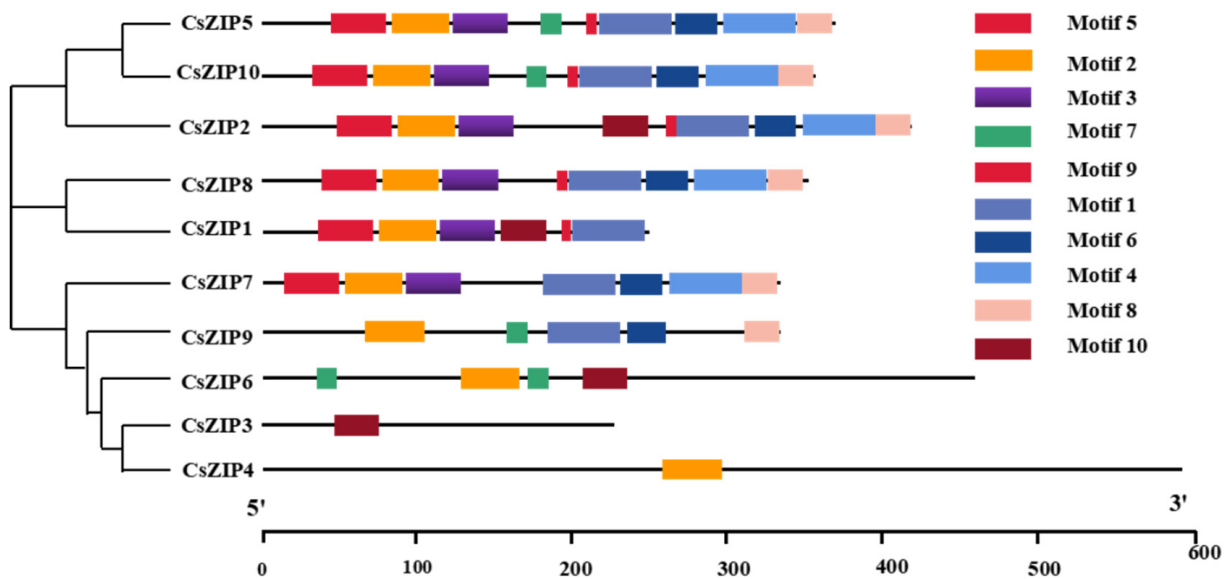


Figure 2. *C. sativus* ZIP proteins exhibit conserved motifs identified by MEME, highlighted with colored boxes.

3.4. Multiple Sequence Alignment

To analyze the characteristics of ZIP protein homologous sequences in comparison to other species, we conducted a comparative study of ZIP proteins in *Arabidopsis*, *Cucumis melo*, *O. sativa*, and *C. sativus*. The transmembrane domains IV-VII exhibited the highest degree of conservation (Figure 3). Previous studies have reported that transmembrane domains IV and V are amphiphilic and play a crucial role in transport, a conclusion that has been further corroborated by subsequent research [47]. In the mutant *irt1*, mutations in the conserved histidine residues or adjacent polar charged residues within transmembrane domains IV and V were found to abolish their transport function [48]. Notably, the IV regions of the sequence alignment in *Arabidopsis*, *Cucumis melo*, *O. sativa*, and *C. sativus* showed the presence of conserved histidine residues (Figure 3).

3.5. Phylogenetic Analysis among Different Species

We obtained a comprehensive understanding of the relative relationship of CsZIP proteins by constructing a phylogenetic tree using the amino acid sequences of ZIP proteins from *Arabidopsis*, *C. sativus*, *Cucumis melo*, and *O. sativa* (Figure 4). The phylogenetic analysis revealed three major clades: Group 1, 2, and 3. In Group 1, there were seven proteins from *Arabidopsis*, three from *C. sativus*, three from *Cucumis melo*, and eight from *O. sativa*. Group 2 consisted of six proteins from *Arabidopsis*, three from *C. sativus*, three from *Cucumis melo*, and three from *O. sativa*. Group 3 included five proteins from *Arabidopsis*, four from *C. sativus*, four from *Cucumis melo*, and five from *O. sativa* (Figure 4). It is worth noting that the number of ZIP proteins varied within each subgroup for *Arabidopsis*, *C. sativus*, *Cucumis melo*, and *O. sativa*. Specifically, half *O. sativa* ZIP proteins were grouped into Group 1, while the distribution among the three clades was relatively equal for the other species. Further investigation within the Group 3 revealed a close relationship between CsZIP6, CmZIP8, AtIAR1, and OsZIP14 (Figure 4). For reference, the amino acid sequences of the ZIP proteins can be found in Dataset S1. This analysis provides valuable insights into the interrelationships of ZIP proteins in different plant species and serves as a foundation for further exploration of their biological functions.

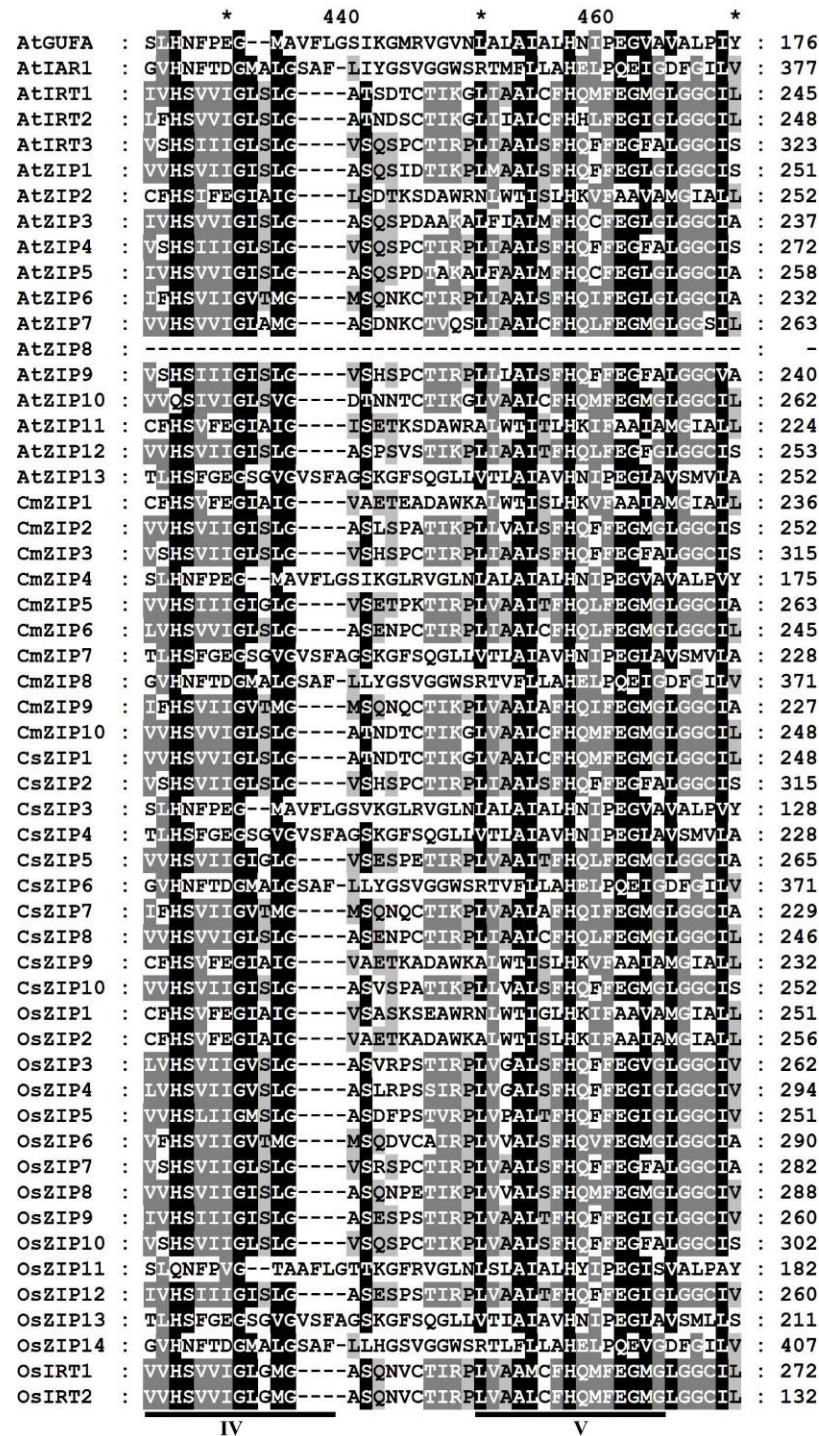


Figure 3. Amino acid sequence alignment for ZIP proteins from *Arabidopsis*, *C. sativus*, *Cucumis melo*, and *O. sativa*. The alignment of ZIP proteins was conducted via MAFFT v.5.3, employing default settings. Black boxes indicate residues that are entirely conserved, while gray boxes highlight residues with a high level of conservation. * represents the positions of the amino acids, which are 430, 450, and 470, respectively.

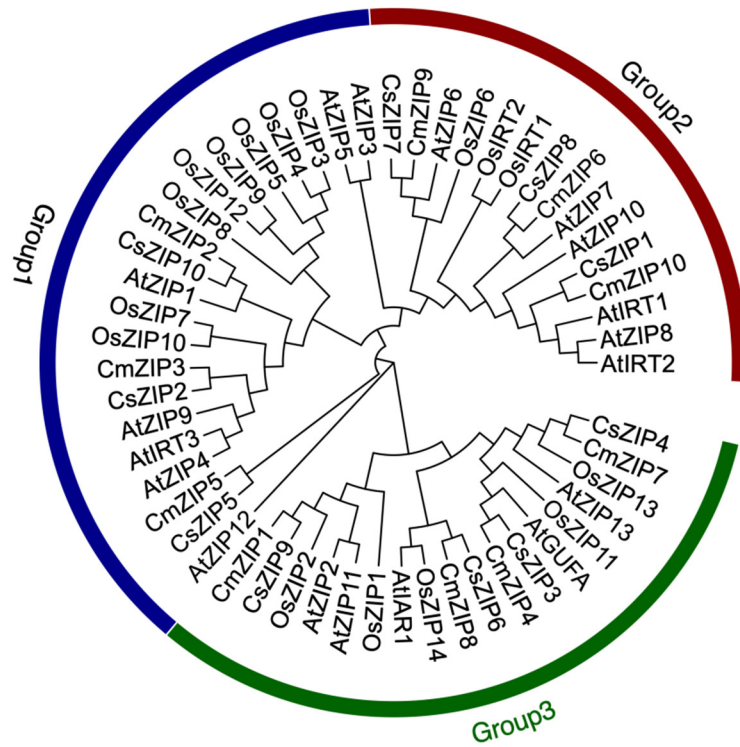


Figure 4. Phylogenetic tree for the ZIP proteins from *Arabidopsis*, *C. sativus*, *Cucumis melo*, and *O. sativa*. In MEGA 7.0, the neighbor-joining (NJ) method was used to construct a root-free amino acid sequence similarity tree, which was repeated 1000 times.

3.6. Chromosome Localization and Collinearity Analysis

The chromosomal distribution analysis of *CsZIP* genes in *C. sativus* revealed an uneven distribution pattern across seven chromosomes (Figure 5). Specifically, three ZIP genes (*CsZIP3*, 4, and 5) were located on chromosome 4, two on each of chromosome 6 and 7, respectively, and one on each of chromosome 1, 2, and 5, and none on chromosome 3 (Figure 5).

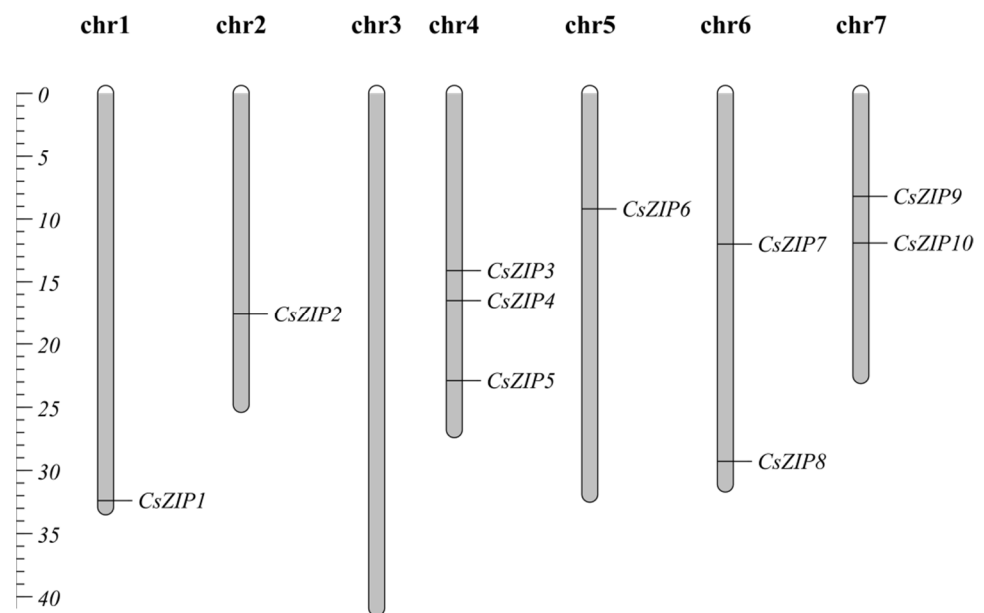


Figure 5. Chromosomal location of *C. sativus* ZIP genes.

We further conducted a collinearity analysis of the ZIP gene family members between *C. sativus* and other plant species, including *Arabidopsis*, *Cucumis melo*, and *O. sativa* (Figure 6). Our results revealed that a total of eight genes were identified to be present in both *C. sativus* and *Arabidopsis*, suggesting a conserved relationship between these two species (Figure 6). In the case of *C. sativus* and *Cucumis melo*, all members of the ZIP gene family exhibited homologous alignment, indicating a high level of homology during the long differentiation process between these two closely related species (Figure 6). However, only two genes showed homology between *C. sativus* and *O. sativa*.

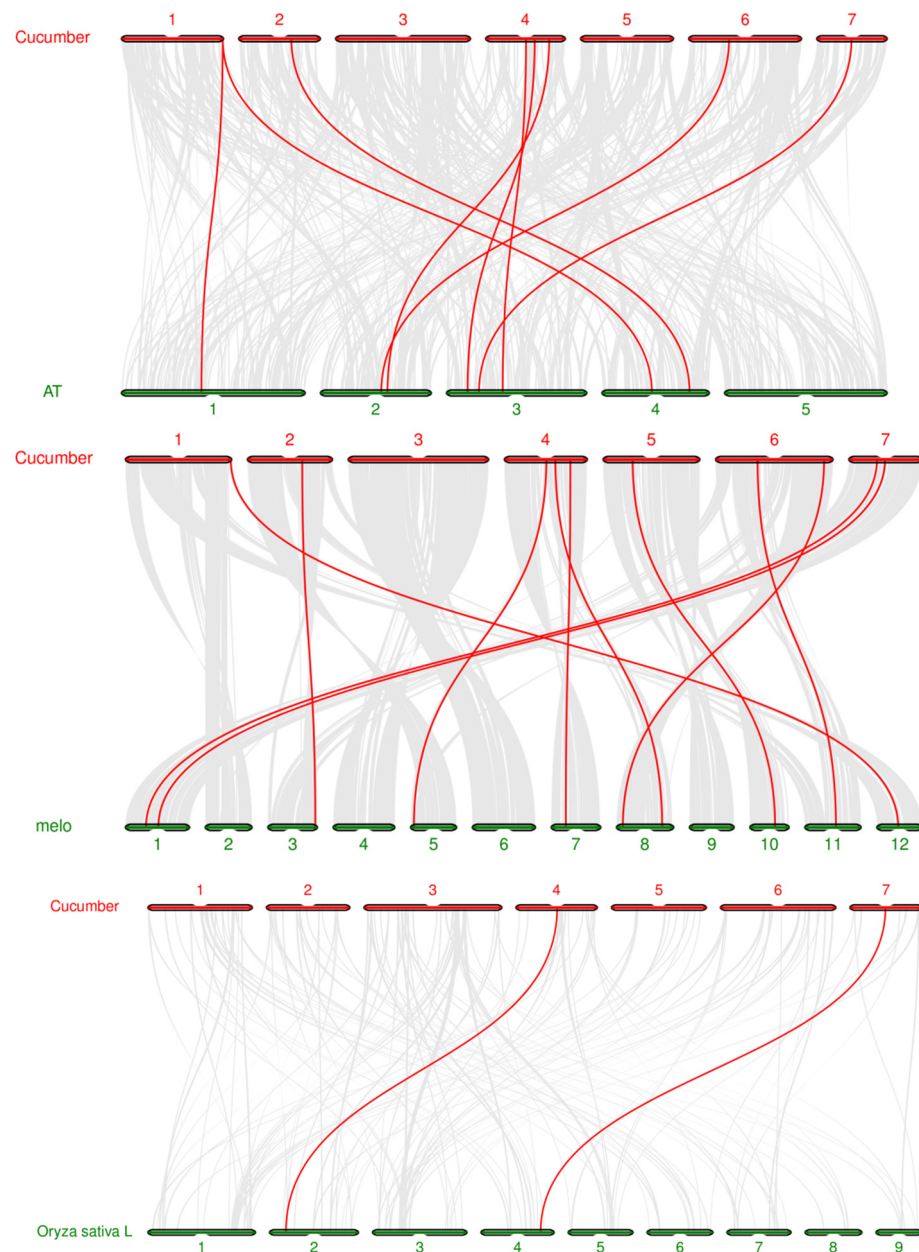


Figure 6. Synteny analysis of ZIPs between *C. sativus* and other plant species (*A. thaliana*, *Oryza sativa*, and *Cucumis melo*): the collinear blocks are marked by gray lines, while the collinear gene pairs with ZIP genes are highlighted by red lines.

3.7. Analysis of Cis-Acting Elements in Promoter Region of CsZIP Genes

The analysis of the 1500 bp sequence upstream of the ZIP gene in *C. sativus* revealed the presence of various *cis*-elements (Figure 7). Specifically, the promoter regions of all the genes in this family contained elements related to some of gibberellin, auxin, salicylic acid,

jasmonic acid, low temperature, and drought stress. Most of the gene promoters contained hormone-related elements, indicating their potential involvement in hormone signaling pathways. Notably, gibberellin-related elements were found in the promoters of several family members, including *CsZIP1*, *CsZIP2*, *CsZIP4*, *CsZIP6*, *CsZIP7*, *CsZIP8*, and *CsZIP10* (Figure 7). This suggests that these genes may play crucial roles in gibberellin-mediated processes. Auxin response elements were predominantly enriched in *CsZIP6*, *CsZIP8*, and *CsZIP10* gene promoters (Figure 7). This finding suggests that these specific genes may be involved in the regulation of plant growth and development through auxin signaling pathways.

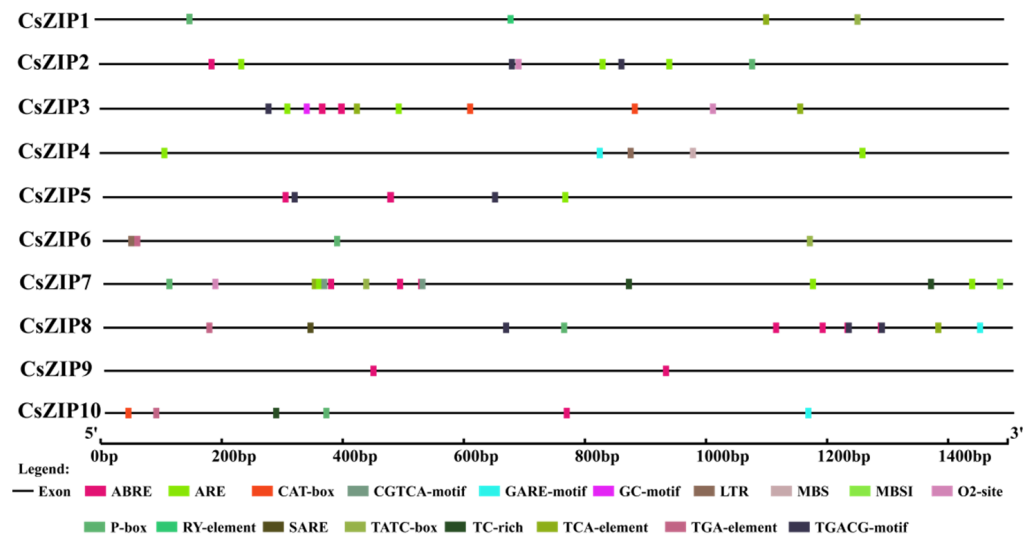


Figure 7. Predicted *cis*-elements in promoter regions of *C. sativus* ZIP genes. The promoter region was defined as a 1.5 kb sequence upstream of the translation initiation codon of the *CsZIP* gene. The *cis*-acting elements were identified utilizing the Plant CARE online tool. Various types of *cis*-acting elements are denoted by distinctively colored closed boxes.

3.8. Expression of *CsZIP* Genes in Different Tissues

This section was dedicated to exploring the functions of ZIP genes in *C. sativus* development by analyzing RNA-seq data derived from various tissues. The expression patterns of *CsZIP* gene family were examined using data from the Cucurbit Genomics Data website and NCBI SAR database, and heat maps were generated to visualize the expression levels across tissues. The results revealed that the expression of ZIP genes in *C. sativus* leaves, stems, and tendrils was relatively lower compared to other tissues (Figure 8a). In contrast, *CsZIP7* and *CsZIP10* showed the highest expression levels in roots, suggesting their possible involvement in regulating ion transport in the underground parts of *C. sativus*. *CsZIP2*, *CsZIP5*, and *CsZIP9* were expressed in flowers, indicating they may play a role in the growth and development of flowers (Figure 8a). On the other hand, *CsZIP1*, *CsZIP3*, *CsZIP4*, *CsZIP6*, and *CsZIP8* exhibited major expression in the ovary, especially *CsZIP3*, *CsZIP4*, and *CsZIP8* displayed high expression levels in the unfertilized ovary (Figure 8a). These findings indicate that these five ZIP genes have regulatory functions in fruit development.

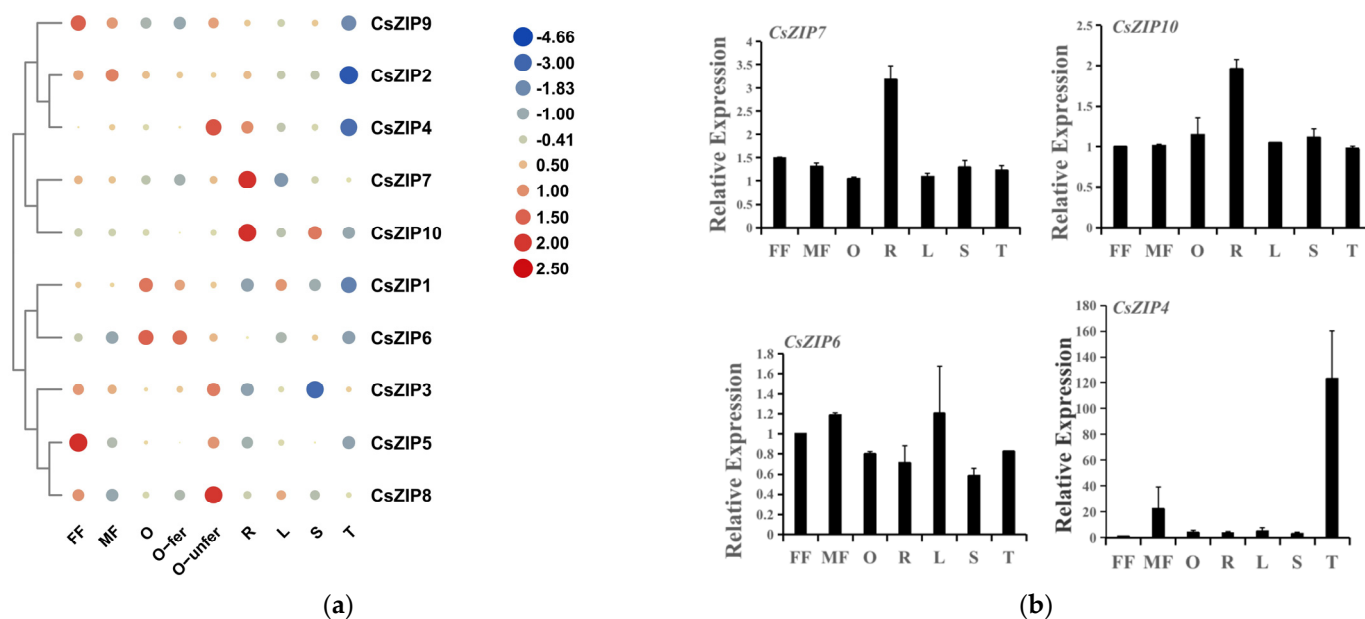


Figure 8. Temporal-spatial expression of *C. sativus* ZIP genes. (a) The heatmap showcases the expression patterns of *CsZIP* genes across nine distinct *C. sativus* tissues. The RNA-seq datasets, acquired via accession number PRJNA80169 from the Cucurbit Genomics Data website, were used. Colors on the scale signify Log₂(FPKM) values, where blue and red represent low and high expression levels, respectively. Detailed FPKM values for *CsZIP* genes can be located in Table S1. (b) Validation of RNA-seq results for four *CsZIP* genes using qRT-PCR. The error bars represent the standard error of the mean ($n = 3$). FF: female flower; R: root; L: leaf; MF: male flower; O-fer: expanded fertilized ovary; S: stem; O: unfertilized ovary; O-unfer: expanded unfertilized ovary; T: tendril.

To further validate the reliability of the RNA-seq results, qRT-PCR analysis of ZIP gene expression in different tissues was performed. Overall, the qRT-PCR results were consistent with the RNA-seq data, confirming the reliability of the datasets (Figure 8b). However, an inconsistency was observed in the expression of *CsZIP4* between male flowers and tendrils, indicating some variations in gene expression in specific tissues (Figure 8b). Therefore, these genes are likely involved in ion transport, flower differentiation, and development, and potentially regulate fruit development.

3.9. Expression Profiles of *CsZIP* Genes under Abiotic and Biotic Stresses

Due to the lack of transcriptomic data on metal ion transport, and in order to enhance our understanding of the functional roles within the ZIP gene family and predict their potential applications in the future, we investigated the impact of various environmental stresses on the expression of *CsZIP* genes, and we assessed their comprehensive expression patterns in response to different stress conditions, including salt, downy mildew (DM, caused by *Pseudoperonospora cubensis*), powdery mildew (PM, caused by *Podosphaera fusca*), and heat, based on publicly available transcriptome data. This analysis enabled us to gain further insights into the potential roles of *CsZIP* genes in mediating plant response to diverse stresses.

Under salt stress, specific expression patterns of *CsZIP* genes were revealed through transcriptome data analysis. *CsZIP4*, *CsZIP5*, *CsZIP6*, and *CsZIP8* genes were up-regulated in response to NaCl treatment; in contrast, *CsZIP1*, *CsZIP3*, and *CsZIP10* genes showed down-regulation (Figure 9a). It is worth noting that Si treatment has been reported to enhance stress resistance and stimulate plant growth. Interestingly, when plants were solely subjected to Si treatment, most *CsZIP* genes exhibited up-regulation in their expression levels. However, the expression of the *CsZIP1* gene was found to be down-regulated (Figure 9a). Additionally, we observed a similar down-regulation of *CsZIP1* gene expression

after exogenous salt and Si treatment. Therefore, it can be concluded that under salt stress conditions, most *CsZIP* genes tend to be up-regulated, while the *CsZIP1* gene specifically demonstrates down-regulation in response to salt stress (Figure 9a).

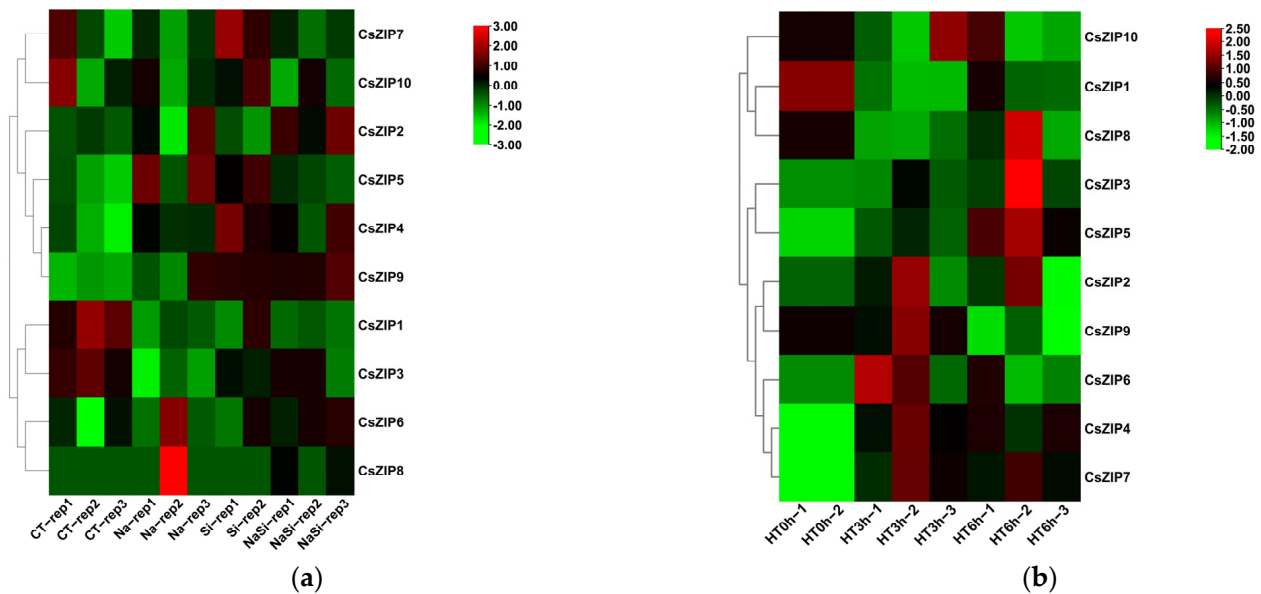


Figure 9. Expression of *CsZIP* genes in response to salt and hot stimuli. (a) Heatmap for displaying the expression profile of *CsZIP* genes in response to salt stresses. (b) The heatmap illustrates the expression patterns of *CsZIP* genes in response to high temperature (42 °C). RNA-seq datasets with accession numbers GSE151055 and GSE116265 were retrieved from the NCBI SAR database. The color scale is representative of $\text{Log}_2(\text{FPKM})$ values, where green signifies low expression, red represents high expression, and black indicates no expression. The FPKM value of *CsZIP* genes under salt and hot treatments are listed in Table S2.

We also examined the response of *CsZIP* genes to heat stress (Figure 9b). At 3 h following exposure to high temperatures, the expression levels of *CsZIP2*, *CsZIP3*, *CsZIP4*, *CsZIP5*, *CsZIP6*, *CsZIP7*, *CsZIP8*, and *CsZIP9* were up-regulated, whereas *CsZIP1* was down-regulated, and similar patterns emerged at 6 h after heat stress, suggesting that these genes may play a crucial role in heat tolerance (Figure 9b).

To explore the role of *CsZIPs* in biotic stress resistance, we conducted an analysis of *CsZIP* expression using the RNA-Seq database. Following inoculation with powdery mildew (PM), we observed distinct gene expression patterns between the susceptible and resistant *C. sativus* lines (Figure 10a). After inoculation with PM, the expression of *CsZIP3*, *CsZIP4*, *CsZIP7*, and *CsZIP9* was down-regulated in both the resistant and susceptible lines. In contrast, the expression of *CsZIP5* was up-regulated (Figure 10a).

For DM inoculation, *CsZIP2*, *CsZIP3*, *CsZIP5*, *CsZIP6*, *CsZIP7*, and *CsZIP9* genes were up-regulated after treatment, while *CsZIP4* genes were down-regulated (Figure 10b).

These findings indicate that *CsZIP* genes are responsive to different environmental stresses and may play diverse roles in mediating plant responses to these stresses. Further research is needed to fully understand the specific functions of each *CsZIP* gene and their contributions to stress resistance in *C. sativus*.

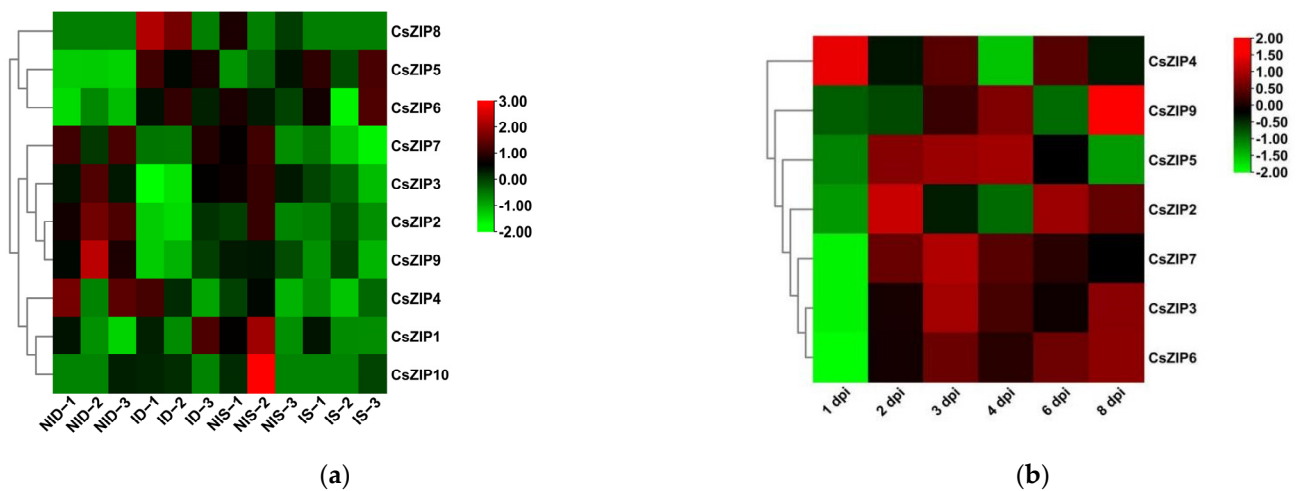


Figure 10. Expression analysis of *CsZIPs* under biotic stresses: The transcriptional levels of *CsZIP* genes after infection with powdery mildew (PM) for 48 h (a) and with downy mildew (DM) for 1–8 days post-inoculation (b) are shown on the heatmaps. The color scale shows increasing expression levels from green to red. ID, PM-inoculated susceptible *C. sativus* line D8 leaves; NID, non-inoculated D8 leaves; IS, PM-inoculated resistant *C. sativus* line SSL508-28 leaves; NIS, non-inoculated SSL508-28 leaves; CT, without inoculation; DPI, days post-inoculation. The FPKM value of *CsZIP* genes under powdery mildew and downy mildew are listed in Table S3.

4. Discussion

The ZIP (ZRT/IRT-like protein) gene family is involved in the absorption and transport of metal ions in plants, playing a crucial role in plant growth, development, and response to heavy metal stress [1]. In this study, a comprehensive genome-wide identification of *CsZIPs* was performed, and a total of 10 genes were identified in *C. sativus*. We further investigated their gene structure, phylogenetic relationship, composition of *cis*-regulatory elements in promoter, chromosome localization, collinearity analysis, and expression patterns under different elemental stresses. These findings enhance our understanding of the ZIP gene family and provide bases for better elucidating the function and evolutionary relationship of *CsZIPs* in *C. sativus*.

Previous studies have reported the identification of the ZIP gene family in various plant species including *A. thaliana*, peanut, and *Populus trichocarpa*. *Arabidopsis* had 15 ZIP members, peanut 30, and *P. trichocarpa* 16 [31,47,49,50]. However, in this study, only 10 *CsZIP* genes were identified (Figure 1). Of the 13 *C. sativus* germplasm resources analyzed, “Cuc80” and “PI183967” contained 9 *CsZIP* genes, whereas the remaining varieties harbored 10 ZIP genes (Table 2). Notably, only *CsZIP10* exhibited a consistent amino acid sequence length, while the lengths of other *CsZIPs* varied among the different varieties (Table 2).

Previous studies have predicted and confirmed the subcellular localization of ZIP proteins. Most ZIP proteins are predicted to be localized in the membrane system. For instance, in *O. sativa*, it has been demonstrated that *OsZIP1*, *OsZIP5*, *OsZIP7*, and *OsZIP8* are localized in the plasma membrane [17,21,22,51]. In peanuts, the endomembrane system is where *AhZIP1.2*, *AhZIP3.2*, *AhZIP3.5*, and *AhZIP7.8* are localized [47]. In *Arabidopsis*, confirmed localization in the plasma membrane has been established for *AtIRT1*, *AtIRT3*, *AtZIP1*, and *AtZIP2* [6,7,19]. In this study, we predicted the subcellular localization of 10 ZIP proteins. The results showed that *CsZIP1*, *CsZIP3*, *CsZIP4*, *CsZIP5*, *CsZIP6*, *CsZIP8*, *CsZIP9*, and *CsZIP10* are predicted to be localized in the cell membrane, with *CsZIP2* and *CsZIP7* in the chloroplast (Table 3).

In the evolutionary process of plant genomes, the emergence of gene family members often accompanies gene duplication, leading to new functions. For example, most of the *AhZIP* genes experienced gene duplication events except *AhIRT1.1/1.3*, *AhZIP7.2/7.8*, and

AhZIP3.5/3.6 [47]. However, unfortunately, we did not detect any gene duplication events in the *CsZIP* genes in *C. sativus*.

The *CsZIP* gene promoters contain many *cis*-acting elements that respond to various hormones and stresses, including gibberellins, methyl jasmonate, abscisic acid, and low temperature. In *S. lycopersicum*, zinc deficiency tolerance is determined by auxin signaling [32]. Furthermore, the response elements of three *ZIP* genes in sunflower are regulated by salicylic acid and methyl jasmonate under iron deficiency [33]. These findings suggest that the expression of *CsZIP* genes can be induced by several plant hormones, such as salicylic acid, MeJA, gibberellins, and auxins. Methyl jasmonate acts as a crucial plant hormone in defense against biotic and abiotic stresses by triggering defense mechanisms and regulating growth [52]. Auxin, on the other hand, controls plant development, with tryptophan being a key amino acid in the auxin synthesis pathway. As Zn participates in tryptophan synthesis, *CsZIP* genes might play a significant role in auxin biosynthesis [53]. Being similar to auxin, gibberellins also regulate various plant growth and development processes, including seed germination and fruit development [54]. Salicylic acid has been shown to greatly enhance plant stress resistance [55]. Additionally, several *cis*-acting elements associated with biotic and abiotic stress responses have been identified in the promoter region of *CsZIP* genes (Figure 7). This suggests that the *CsZIP* gene family may adapt to different environmental stresses through hormone signals.

In general, the expression patterns of genes are correlated with their functions [51]. The expression data of *CsZIPs* in different tissues provide valuable insights into the possible functions of the *ZIP* gene family. Previous studies have confirmed that *ZIP* genes are predominantly expressed in roots, regardless of the plant species, such as *Arabidopsis*, *O. sativa*, or barley, with many genes being induced under deficiencies of environmental zinc or other metallic elements [7,19,56,57]. Existing research has indicated that within tomatoes, the *SZIP* gene family comprises 15 members, with 13 expressing in the roots, exhibiting significantly high expression levels. Among these, 11 *SZIP* genes are expressed in fruits, albeit with varying expression across different developmental stages, indicating the involvement of *SZIP* genes in the accumulation of zinc and iron in *S. lycopersicum* fruits or their redistribution among different tissues [58]. Similarly, *CsZIP7* and *CsZIP10* exhibit high expression in *C. sativus* roots, while *CsZIP10* has higher expression levels in stems compared to other tissues (Figure 8). This suggests that *CsZIP7* and *CsZIP10* may play functional roles in these two tissues. Furthermore, it was observed that *CsZIP2*, *CsZIP5*, and *CsZIP9* show higher expression levels in flowers, while *CsZIP3*, *CsZIP4*, and *CsZIP8* exhibit the highest expression levels in fertilized ovaries. *CsZIP1* and *CsZIP6* are also expressed in ovaries (Figure 8). Based on this information, it can be inferred that these *CsZIP* genes may participate in the regulation of fruit development by regulating the accumulation of Zn and Fe or their redistribution among different tissues.

Previous studies have primarily focused on the regulatory roles of *ZIP* genes in plant metal ion uptake and transport. For instance, *AtZIP3* is known to play a crucial role in facilitating the absorption of Zn and Fe from the soil into plant roots [8]. On the other hand, *AtZIP2* functions by mediating the uptake of Mn/Zn into the parenchyma cells of the xylem, thereby enabling the efficient transportation of Mn/Zn to the aboveground parts of plants [7]. However, in this study, we found that *CsZIP* genes could respond to different environmental stresses. We investigated the expression of *CsZIP* genes under different environmental stresses, including powdery mildew, downy mildew, salt, and heat. The results showed differential expression of *CsZIP* genes in response to high temperature (Figure 9b), salt, silicon (Figure 9a), powdery mildew (Figure 10a), and downy mildew treatments (Figure 10a). These results provide valuable clues suggesting that *CsZIP* genes may have significant functions in multiple stress conditions. The functionality and regulatory mechanisms of the *CsZIP* gene family will require further validation in the future, particularly regarding their functional responses under different environmental stressors. Utilizing gene-editing technologies such as CRISPR-Cas9 to generate mutants

will help explore the precise roles of CsZIP genes in plant growth, development, and stress responses. Further investigations into the regulatory mechanisms of the CsZIP gene family, encompassing transcriptional, translational, and post-transcriptional regulations, will provide a deeper understanding of these genes' functions across various biological processes. These potential future research directions will contribute to a more comprehensive elucidation of the significance of the CsZIP gene family in plants, thereby enhancing our understanding of regulatory mechanisms governing plant adaptability and stress resilience.

5. Conclusions

In this study, we performed a pan-genome-wide identification of the ZIP gene family in *C. sativus*. A total of 10 members were identified. Eleven of the thirteen accessions contained all the CsZIP genes. The ZIP gene family has three evolutionary branches and contains conserved histidine residues. The CsZIP gene promoters contained elements that responded to plant hormone signaling pathways, indicating that plant hormone signals may have an impact on CsZIP-mediated biotic and abiotic stresses. The expression patterns of CsZIPs in different tissues showed that the CsZIP gene family may be related to the growth and development of *C. sativus*. Finally, CsZIPs could respond to different environmental stresses. In summary, this study helps to improve the current understanding of the CsZIP gene family and provides a basis for exploring their functions in *C. sativus*.

Supplementary Materials: The following supporting information can be downloaded at: <https://www.mdpi.com/article/10.3390/agriculture14010133/s1>, Figure S1: The conserved motif LOGO of *C. sativus* ZIP proteins; Table S1: The FPKM values of CsZIP genes; Table S2: The FPKM value of CsZIP genes under salt and hot treatments; Table S3: The FPKM value of CsZIP genes under powdery mildew and downy mildew; Table S4: The primer sequences used for the qRT-PCR; Dataset S1: The amino acid sequences of the ZIP proteins. Dataset S2: All CsZIP protein sequences of 13 *C. sativus* accessions.

Author Contributions: Conceptualization, Z.R.; methodology, Z.W. and M.Y.; software, Z.W., X.W. and J.C.; validation, Z.W.; formal analysis, Z.W., M.Y. and J.H.; investigation, Z.W. and J.H.; resources, Z.R. and L.W.; data curation, Z.W.; writing—original draft preparation, Z.W. and Z.R.; writing—review and editing, L.W. and Z.R.; visualization, L.W. and Z.R.; supervision, L.W. and Z.R.; project administration, L.W. and Z.R.; funding acquisition, Z.W. and Z.R. All authors have read and agreed to the published version of the manuscript.

Funding: This research was funded by the National Natural Science Foundation of China (31972419 and 32172605), the Agricultural Variety Improvement Project of Shandong Province (2022LZGCQY001), and the “Taishan Scholar” Foundation of the People’s Government of Shandong Province (ts20130932).

Institutional Review Board Statement: Not applicable.

Data Availability Statement: The data presented in this study are available in this article and Supplementary Materials.

Acknowledgments: We extend our appreciation to the anonymous reviewers for their valuable suggestions to help improve this article.

Conflicts of Interest: The authors declare no conflicts of interest.

References

1. Grotz, N.; Guerinot, M.L. Molecular aspects of Cu, Fe and Zn homeostasis in plants. *Biochim. Biophys. Acta* **2006**, *1763*, 595–608. [[CrossRef](#)] [[PubMed](#)]
2. Guerinot, M.L. The ZIP family of metal transporters. *Biochim. Biophys. Acta* **2000**, *1465*, 190–198. [[CrossRef](#)] [[PubMed](#)]
3. Gaither, L.A.; Eide, D.J. Eukaryotic zinc transporters and their regulation. *Biometals* **2001**, *14*, 251–270. [[CrossRef](#)]
4. Nishida, S.; Tsuzuki, C.; Kato, A.; Aisu, A.; Yoshida, J.; Mizuno, T. AtIRT1, the primary iron uptake transporter in the root, mediates excess nickel accumulation in *Arabidopsis thaliana*. *Plant Cell Physiol.* **2011**, *52*, 1433–1442. [[CrossRef](#)] [[PubMed](#)]

5. Krausko, M.; Labajová, M.; Peterková, D.; Jásik, J. Specific expression of AtIRT1 in phloem companion cells suggests its role in iron translocation in aboveground plant organs. *Plant Signal. Behav.* **2021**, *16*, 1925020. [[CrossRef](#)] [[PubMed](#)]
6. Vert, G.; Barberon, M.; Zelazny, E.; Séguéla, M.; Briat, J.F.; Curie, C. *Arabidopsis* IRT2 cooperates with the high-affinity iron uptake system to maintain iron homeostasis in root epidermal cells. *Planta* **2009**, *229*, 1171–1179. [[CrossRef](#)]
7. Milner, M.J.; Seamon, J.; Craft, E.; Kochian, L.V. Transport properties of members of the ZIP family in plants and their role in Zn and Mn homeostasis. *J. Exp. Bot.* **2013**, *64*, 369–381. [[CrossRef](#)]
8. Gaitán-Solís, E.; Taylor, N.J.; Siritunga, D.; Stevens, W.; Schachtman, D.P. Overexpression of the transporters AtZIP1 and AtMTP1 in cassava changes zinc accumulation and partitioning. *Front. Plant Sci.* **2015**, *6*, 492. [[CrossRef](#)]
9. Ramegowda, Y.; Venkategowda, R.; Jagadish, P. Expression of a rice Zn transporter, OsZIP1, increases Zn concentration in tobacco and finger millet transgenic plants. *Plant Biotechnol. Rep.* **2013**, *7*, 309–319. [[CrossRef](#)]
10. Van de Mortel, J.E.; Almar Villanueva, L.; Schat, H.; Kwekkeboom, J.; Coughlan, S.; Moerland, P.D.; Ver Loren van Themaat, E.; Koornneef, M.; Aarts, M.G. Large expression differences in genes for iron and zinc homeostasis, stress response, and lignin biosynthesis distinguish roots of *Arabidopsis thaliana* and the related metal hyperaccumulator *Thlaspi caerulescens*. *Plant Physiol.* **2006**, *142*, 1127–1147. [[CrossRef](#)]
11. Itai, R.N.; Ogo, Y.; Kobayashi, T.; Nakanishi, H.; Nishizawa, N.K. rice genes involved in phytosiderophore biosynthesis are synchronously regulated during the early stages of iron deficiency in roots. *Rice* **2013**, *6*, 16. [[CrossRef](#)] [[PubMed](#)]
12. Ishimaru, Y.; Suzuki, M.; Tsukamoto, T.; Suzuki, K.; Nakazono, M.; Kobayashi, T.; Wada, Y.; Watanabe, S.; Matsushashi, S.; Takahashi, M.; et al. Rice plants take up iron as an Fe³⁺-phytosiderophore and as Fe²⁺. *Plant J.* **2006**, *45*, 335–346. [[CrossRef](#)] [[PubMed](#)]
13. Lee, S.; An, G. Over-expression of OsIRT1 leads to increased iron and zinc accumulations in rice. *Plant Cell Environ.* **2009**, *32*, 408–416. [[CrossRef](#)] [[PubMed](#)]
14. Nakanishi, H.; Ogawa, I.; Ishimaru, Y.; Mori, S.; Nishizawa, N.K. Iron deficiency enhances cadmium uptake and translocation mediated by the Fe²⁺ transporters OsIRT1 and OsIRT2 in rice. *Soil. Sci. Plant Nutr.* **2006**, *52*, 464–469. [[CrossRef](#)]
15. Ishimaru, Y.; Kim, S.; Tsukamoto, T.; Oki, H.; Kobayashi, T.; Watanabe, S.; Matsushashi, S.; Takahashi, M.; Nakanishi, H.; Mori, S.; et al. Mutational reconstructed ferric chelate reductase confers enhanced tolerance in rice to iron deficiency in calcareous soil. *Proc. Natl. Acad. Sci. USA* **2007**, *104*, 7373–7378. [[CrossRef](#)]
16. Liu, X.S.; Feng, S.J.; Zhang, B.Q.; Wang, M.Q.; Cao, H.W.; Rono, J.K.; Chen, X.; Yang, Z.M. OsZIP1 functions as a metal efflux transporter limiting excess zinc, copper and cadmium accumulation in rice. *BMC Plant Biol.* **2019**, *19*, 283. [[CrossRef](#)]
17. Shimaru, Y.; Masuda, H.; Suzuki, M.; Bashir, K.; Takahashi, M.; Nakanishi, H.; Mori, S.; Nishizawa, N.K. Overexpression of the OsZIP4 zinc transporter confers disarrangement of zinc distribution in rice plants. *J. Exp. Bot.* **2007**, *58*, 2909–2915. [[CrossRef](#)]
18. Lee, S.; Jeong, H.J.; Kim, S.A.; Lee, J.; Guerinot, M.L.; An, G. OsZIP5 is a plasma membrane zinc transporter in rice. *Plant Mol. Biol.* **2010**, *73*, 507–517. [[CrossRef](#)]
19. Lee, S.; Kim, S.A.; Lee, J.; Guerinot, M.L.; An, G. Zinc deficiency-inducible OsZIP8 encodes a plasma membrane-localized zinc transporter in rice. *Mol. Cells* **2010**, *29*, 551–558. [[CrossRef](#)]
20. Wu, X.; Zhu, Z.B.; Chen, J.H.; Huang, Y.F.; Liu, Z.L.; Zou, J.W.; Chen, Y.H.; Su, N.N.; Cui, J. Transcriptome analysis revealed pivotal transporters involved in the reduction of cadmium accumulation in pak choi (*Brassica chinensis* L.) by exogenous hydrogen-rich water. *Chemosphere* **2019**, *216*, 684–697. [[CrossRef](#)]
21. Guo, J.; Li, K.; Zhang, X.; Huang, H.; Huang, F.; Zhang, L.; Wang, Y.; Li, T.; Yu, H. Genetic properties of cadmium translocation from straw to brown rice in low-grain cadmium rice line. *Ecotoxicol. Environ. Saf.* **2019**, *182*, 109422. [[CrossRef](#)] [[PubMed](#)]
22. Yu, R.; Li, D.; Du, X.; Xia, S.; Liu, C.; Shi, G. Comparative transcriptome analysis reveals key cadmium transport-related genes in roots of two pak choi (*Brassica rapa* L. ssp. *chinensis*) cultivars. *BMC Genom.* **2017**, *18*, 587. [[CrossRef](#)] [[PubMed](#)]
23. Bienert, S.; Waterhouse, A.; Beer, T.A.; Tauriello, G.; Studer, G.; Bordoli, L.; Schwede, T. The SWISS-MODEL Repository—new features and functionality. *Nucleic Acids Res.* **2017**, *45*, D313–D319. [[CrossRef](#)] [[PubMed](#)]
24. Fan, W.; Liu, C.; Cao, B.; Qin, M.; Long, D.; Xiang, Z.; Zhao, A. Genome-Wide Identification and Characterization of Four Gene Families Putatively Involved in Cadmium Uptake, Translocation and Sequestration in Mulberry. *Front. Plant Sci.* **2018**, *9*, 879. [[CrossRef](#)]
25. Palusińska, M.; Barabasz, A.; Kozak, K.; Papierniak, A.; Maślińska, K.; Antosiewicz, D.M. Zn/Cd status-dependent accumulation of Zn and Cd in root parts in tobacco is accompanied by specific expression of ZIP genes. *BMC Plant Biol.* **2020**, *20*, 37. [[CrossRef](#)] [[PubMed](#)]
26. Alamholo, M.; Tarinejad, A. Molecular mechanism of drought stress tolerance in barley (*Hordeum vulgare* L.) via a combined analysis of the transcriptome data. *Czech J. Genet. Plant Breed.* **2023**, *59*, 76–94. [[CrossRef](#)]
27. Wang, L.; Xu, Z.; Yin, W.; Xu, K.; Wang, S.; Shang, Q.; Sa, W.; Liang, J.; Wang, L. Genome-wide analysis of the Thaumatin-like gene family in Qingke (*Hordeum vulgare* L. var. *nudum*) uncovers candidates involved in plant defense against biotic and abiotic stresses. *Front. Plant Sci.* **2022**, *13*, 912296. [[CrossRef](#)]
28. Zheng, S.; Dai, H.; Meng, Q.; Huang, R.; Tong, H.; Yuan, L. Identification and expression analysis of the ZRT, IRT-like protein (ZIP) gene family in *Camellia sinensis* (L.) O. Kuntze. *Plant Physiol. Biochem.* **2022**, *172*, 87–100. [[CrossRef](#)]
29. Si, Z.; Qiao, Y.; Zhang, K.; Ji, Z.; Han, J. Characterization of Nucleotide Binding -Site-Encoding Genes in Sweetpotato, *Ipomoea batatas* (L.) Lam., and Their Response to Biotic and Abiotic Stresses. *Cytogenet. Genome Res.* **2021**, *161*, 257–271. [[CrossRef](#)]

30. Song, X.; Li, E.; Song, H.; Du, G.; Li, S.; Zhu, H.; Chen, G.; Zhao, C.; Qiao, L.; Wang, J.; et al. Genome-wide identification and characterization of nonspecific lipid transfer protein (nsLTP) genes in *Arachis duranensis*. *Genomics* **2020**, *112*, 4332–4341. [[CrossRef](#)]
31. Vert, G.; Grotz, N.; Dédaldéchamp, F.; Gaymard, F.; Guerinot, M.L.; Briat, J.F.; Curie, C. IRT1, an *Arabidopsis* transporter essential for iron uptake from the soil and for plant growth. *Plant Cell* **2002**, *14*, 1223–1233. [[CrossRef](#)] [[PubMed](#)]
32. Akther, M.S.; Das, U.; Tahura, S.; Prity, S.A.; Islam, M.; Kabir, A.H. Regulation of Zn uptake and redox status confers Zn deficiency tolerance in tomato. *Sci. Hortic.* **2020**, *273*, 109624. [[CrossRef](#)]
33. Kabir, A.H.; Tahura, S.; Elseehy, M.M.; El-Shehawi, A.M. Molecular characterization of Fe-acquisition genes causing decreased Fe uptake and photosynthetic inefficiency in Fe-deficient sunflower. *Sci. Rep.* **2021**, *11*, 5537. [[CrossRef](#)]
34. Liu, M.; Zhang, C.; Duan, L.; Luan, Q.; Li, J.; Yang, A.; Qi, X.; Ren, Z. CsMYB60 is a key regulator of flavonols and proanthocyanidins that determine the colour of fruit spines in cucumber. *J. Exp. Bot.* **2019**, *70*, 69–84. [[CrossRef](#)] [[PubMed](#)]
35. Chou, K.C.; Shen, H.B. Cell-PLoc: A package of Web servers for predicting subcellular localization of proteins in various organisms. *Nat. Protoc.* **2008**, *3*, 153–162. [[CrossRef](#)]
36. Hu, B.; Jin, J.; Guo, A.Y.; Zhang, H.; Luo, J.; Gao, G. GSDS 2.0: An upgraded gene feature visualization server. *Bioinformatics* **2015**, *31*, 1296–1297. [[CrossRef](#)] [[PubMed](#)]
37. Bailey, T.L.; Williams, N.; Misleh, C.; Li, W.W. MEME: Discovering and analyzing DNA and protein sequence motifs. *Nucleic Acids Res.* **2006**, *34*, W369–W373. [[CrossRef](#)]
38. Crooks, G.E.; Hon, G.; Chandonia, J.M.; Brenner, S.E. WebLogo: A sequence logo generator. *Genome Res.* **2004**, *14*, 1188–1190. [[CrossRef](#)]
39. Voorrips, R.E. MapChart: Software for the graphical presentation of linkage maps and QTLs. *J. Hered.* **2002**, *93*, 77–78. [[CrossRef](#)]
40. Li, L.; Stoeckert, C.J., Jr.; Roos, D.S. OrthoMCL: Identification of ortholog groups for eukaryotic genomes. *Genome Res.* **2003**, *13*, 2178–2189. [[CrossRef](#)]
41. Krzywinski, M.; Schein, J.; Birol, I.; Connors, J.; Gascoyne, R.; Horsman, D.; Jones, S.J.; Marra, M.A. Circos: An information aesthetic for comparative genomics. *Genome Res.* **2009**, *19*, 1639–1645. [[CrossRef](#)]
42. Koch, M.A.; Haubold, B.; Mitchell-Olds, T. Comparative evolutionary analysis of chalcone synthase and alcohol dehydrogenase loci in *Arabidopsis*, *Arabis*, and related genera (Brassicaceae). *Mol. Biol. Evol.* **2000**, *17*, 1483–1498. [[CrossRef](#)] [[PubMed](#)]
43. Lescot, M.; Déhais, P.; Thijs, G.; Marchal, K.; Moreau, Y.; Van de Peer, Y.; Rouzé, P.; Rombauts, S. PlantCARE, a database of plant *cis*-acting regulatory elements and a portal to tools for in silico analysis of promoter sequences. *Nucleic Acids Res.* **2002**, *30*, 325–327. [[CrossRef](#)] [[PubMed](#)]
44. Chen, C.; Chen, H.; Zhang, Y.; Thomas, H.R.; Frank, M.H.; He, Y.; Xia, R. TBtools: An Integrative Toolkit Developed for Interactive Analyses of Big Biological Data. *Mol. Plant* **2020**, *13*, 1194–1202. [[CrossRef](#)] [[PubMed](#)]
45. Livak, K.J.; Schmittgen, T.D. Analysis of relative gene expression data using real-time quantitative PCR and the 2^{(-Delta Delta C(T))} Method. *Methods* **2001**, *25*, 402–408. [[CrossRef](#)]
46. Li, H.; Wang, S.; Chai, S.; Yang, Z.; Zhang, Q.; Xin, H.; Xu, Y.; Lin, S.; Chen, X.; Yao, Z.; et al. Graph-based pan-genome reveals structural and sequence variations related to agronomic traits and domestication in cucumber. *Nat. Commun.* **2022**, *13*, 682. [[CrossRef](#)]
47. Zhang, Z.; Chen, N.; Zhang, Z.; Shi, G. Genome-Wide Identification and Expression Profile Reveal Potential Roles of Peanut ZIP Family Genes in Zinc/Iron-Deficiency. *Toler. Plants* **2022**, *11*, 786. [[CrossRef](#)]
48. Eng, B.H.; Guerinot, M.L.; Eide, D.; Saier, M.H., Jr. Sequence analyses and phylogenetic characterization of the ZIP family of metal ion transport proteins. *J. Membr. Biol.* **1998**, *166*, 1–7. [[CrossRef](#)]
49. Fu, X.Z.; Zhou, X.; Xing, F.; Ling, L.L.; Chun, C.P.; Cao, L.; Aarts, M.G.M.; Peng, L.Z. Genome-Wide Identification, Cloning and Functional Analysis of the Zinc/Iron-Regulated Transporter-Like Protein (ZIP) Gene Family in Trifoliolate Orange (*Poncirus trifoliata* L. Raf.). *Front. Plant Sci.* **2017**, *8*, 588. [[CrossRef](#)]
50. Zhang, H.; Zhao, S.; Li, D. Genome-Wide Analysis of the ZRT, IRT-Like Protein (ZIP) Family and Their Responses to Metal Stress in *Populus trichocarpa*. *Plant Mol. Biol. Rep.* **2017**, *35*, 534–549. [[CrossRef](#)]
51. Li, S.; Liu, X.; Zhou, X.; Li, Y.; Yang, W.; Chen, R. Improving Zinc and Iron Accumulation in Maize Grains Using the Zinc and Iron Transporter ZmZIP5. *Plant Cell Physiol.* **2019**, *60*, 2077–2085. [[CrossRef](#)] [[PubMed](#)]
52. Cheong, J.J.; Choi, Y.D. Methyl jasmonate as a vital substance in plants. *Trends Genet.* **2003**, *19*, 409–413. [[CrossRef](#)]
53. Castillo-Gonzalez, J.; Ojeda-Barrios, D.; Hernandez-Rodriguez, A.; Gonzalez-Franco, A.C.; Robles-Hernandez, L.; Lopez-Ochoa, G.R. ZINC METALLOENZYMES IN PLANTS. *Interciencia* **2018**, *43*, 242–248.
54. Eriksson, S.; Böhlenius, H.; Moritz, T.; Nilsson, O. GA4 is the active gibberellin in the regulation of LEAFY transcription and *Arabidopsis* floral initiation. *Plant Cell* **2006**, *18*, 2172–2181. [[CrossRef](#)]
55. Preciado-Rangel, P.; Reyes-Pérez, J.J.; Ramírez-Rodríguez, S.C.; Salas-Pérez, L.; Fortis-Hernández, M.; Murillo-Amador, B.; Troyo-Diéguez, E. Foliar Aspersions of Salicylic Acid Improves Phenolic and Flavonoid Compounds, and Also the Fruit Yield in Cucumber (*Cucumis sativus* L.). *Plants* **2019**, *8*, 44. [[CrossRef](#)] [[PubMed](#)]
56. Pedas, P.; Schjoerring, J.K.; Husted, S. Identification and characterization of zinc-starvation-induced ZIP transporters from barley roots. *Plant Physiol. Biochem.* **2009**, *47*, 377–383. [[CrossRef](#)]

57. Wintz, H.; Fox, T.; Wu, Y.Y.; Feng, V.; Chen, W.; Chang, H.S.; Zhu, T.; Vulpe, C. Expression profiles of *Arabidopsis thaliana* in mineral deficiencies reveal novel transporters involved in metal homeostasis. *J. Biol. Chem.* **2003**, *278*, 47644–47653. [[CrossRef](#)]
58. Gong, Y.; Zhao, L.; Yan, F. Genome-Wide Identification and Expression Pattern Analysis of the Tomato ZIP Gene Family. *Northeast. Agric. Sci.* **2023**, *48*, 42–48+109. [[CrossRef](#)]

Disclaimer/Publisher’s Note: The statements, opinions and data contained in all publications are solely those of the individual author(s) and contributor(s) and not of MDPI and/or the editor(s). MDPI and/or the editor(s) disclaim responsibility for any injury to people or property resulting from any ideas, methods, instructions or products referred to in the content.